IEEE Access
Multidisciplinary | Rapid Review | Open Access Journal

Received January 24, 2020, accepted February 8, 2020, date of publication February 13, 2020, date of current version February 24, 2020.

Digital Object Identifier 10.1109/ACCESS.2020.2973709

Combined Noise and Clock CRLB Error Model for the Optimization of Node Location in Time Positioning Systems

RUBÉN ÁLVAREZ[1], JAVIER DÍEZ-GONZALEZ[2], LIDIA SÁNCHEZ-GONZÁLEZ[2], AND HILDE PEREZ[2]

[1]Positioning Department, Drotium, Universidad de León, 24071 León, Spain
[2]Department of Mechanical, Computer and Aerospace Engineering, Universidad de León, 24071 León, Spain

Corresponding authors: Rubén Álvarez (ruben.alvarez@drotium.com) and Javier Díez-Gonzalez (jdieg@unileon.es)

This work was supported by the Spanish Ministry of Economy, Industry and Competitiveness under Grant DPI2016-79960-C3-2-P.

ABSTRACT The emergence of autonomous vehicles with high needs for accuracy in location has hardened the requirements of the positioning systems used for navigation. Local Positioning Systems (LPS) have shown an excellent adaptation to these conditions, thanks to stability and reduction in the levels of positioning uncertainty. The accuracy achieved by methodologies based on temporal measurements depends mainly on the uncertainties in the measurements of these systems. In this aspect, the presence of noise and the existence of temporary instabilities in measurement clocks, depending on the distribution of sensors in the environment, acquire great relevance. In this article, we introduce for the first time in the authors' best knowledge a Cramér-Rao Lower Bound (CRLB) model for the quantification of the global uncertainty in positioning systems caused by both noise and temporary instabilities in the measurement devices. Additionally, this technique is applied to the optimization of sensor distributions for Time of Arrival (TOA), Time Difference of Arrival (TDOA) and Asynchronous TDOA (A-TDOA) architectures using a Genetic Algorithm in a non-uniform 3D environment. Results show that A-TDOA methodology significantly overcomes synchronous architectures in terms of global accuracy and stability when noise and clock errors are considered in time measurements of LPS applications.

INDEX TERMS Clock instability, CRLB, genetic algorithm, global accuracy, LPS, noise.

I. INTRODUCTION

The spatial location of objects in real-time has become one of the main factors of progress in current technological development. Its influence in relevant areas of modern society, such as transport, industry and security, is particularly noteworthy.

Over the last few years, the emergence of autonomous vehicles has increased the accuracy and availability needs of the positioning systems as an essential part for the proper functioning and controlled navigation of these new devices through wireless communications. This dependence causes a remarkable hardening in the requirements of the positioning systems of these modern applications.

Traditionally, two main conceptions in the positioning systems design have been considered: a global coverage of the system through satellites in space trying to offer the maximum availability, or a local deployment of sensors looking for a particular adaptation to the characteristics of the environment and the positioning targets inside a known area.

Global Navigation Satellite Systems (GNSS) have represented a great advance in the history of humanity in terms of navigation. The deployment of constellations of satellites in space allows the global coverage of their signals extending even the use of the systems to difficult accessible environments. However, they present serious drawbacks when it comes to providing a stable navigation service with high accuracy services under real operating conditions. The reasons lie in the high probability of appearance of disruptive phenomena along the positioning signals path, due to the great distance between the satellites and the objects to be positioned.

The associate editor coordinating the review of this manuscript and approving it for publication was Woorham Bae.

The problem associated with GNSS is solved through Local Positioning Systems (LPS). These systems are built on the conception of an infrastructure of terrestrial sensors in charge of making the necessary measurements for the location. This approach entails a notable reduction in terms of the distance of the path of the positioning signal, favoring the reduction of harmful phenomena which may affect the accuracy of system measurements. Additionally, the flexibility in the location of sensors offers the advantage of adapting the system to the terrestrial orography taken into account the operating conditions of the environment, thereby increasing the position accuracy.

Regardless of the type of wireless system selected, GNSS or LPS, the location of objects requires the treatment of signals to define the position of any target in space. The systems act through the processing of signals emitted by the target, the satellites or nodes [1]. If this signal is processed inside the target, the systems are classified as active or direct while if the signal is treated in the positioning infrastructure the systems are known as passive or indirect.

These systems depend on the acquisition of some measurements of signal and physical properties such as time, angle, power, frequency or phase to determine the location of the targets.

Time systems such as the Time of Arrival (TOA) [2] and Time Difference of Arrival (TDOA) [3] relies on the time-of-flight of the signal between an emitter and a receiver. Angle of Arrival (AOA) [4] measures the angle of an emission with respect to known position references. Received Signal Strength Indication (RSSI) [5] relies on the deterioration of the signal power in its propagation while acoustic Doppler-based systems [6] measure the differences in frequency of the signal among a set of receivers. Recent studies are also starting to combine these methods with sensor fusion [7] and including the use of multiple phase delays among the signals in Phase Difference of Arrival (PDOA) methods [8], [9].

Among all of these wireless methods, those based on temporary measurements -TOA and TDOA- stand out mainly due to their high ratio between accuracy, provided by the methodology, and the complexity associated with architecture.

The main source of error comes from the necessary temporal synchronization between sensors in the TOA and TDOA architectures which acquires special relevance in LPS due to the higher sensitivity needs in the measurements and the increased accuracy requirements.

However, there is a difference between TOA and TDOA systems. While TOA systems require the synchronism of the clocks of every sensor involved in the localization process, TDOA systems do not require this synchronism as they measure relative times of flight.

Nevertheless, the errors associated with the synchronization process in both systems are no longer negligible due to the reduction in the magnitude of the temporary measurement, making it difficult to implement these methodologies in applications with high location accuracy [10], [11].

The solution goes through the introduction of TDOA architectures of asynchronous typology, built on the basis of reduction or elimination of synchronization between the sensors of the system by centralizing all the system measurements in a single clock of a coordinator sensor. Within these systems, the Asynchronous TDOA (A-TDOA) [12] and Difference-time TDOA (D-TDOA) [13] architectures stand out. In one of our previous works [14] we perform a comparison in terms of accuracy for these methodologies in 3D environments, obtaining the best overall results for the A-TDOA architecture. For this reason, in this article a comparison between synchronous (TOA and TDOA) and asynchronous temporal methods (A-TDOA) will be addressed. This will allow us to determine the influence of the synchronization process on the global positioning error of the systems.

However, in order to achieve valuable results, the synchronization error cannot be addressed separately from other error sources in a direct approach. Although the uncertainties linked to the temporal measurements are the main source of error in time positioning systems, this only happens when other factors are optimized. For instance, in the positioning design, the selection of the architecture and algorithms for the location determination lay down the first thresholds of uncertainty in the calculation of the position [15].

After this consideration, the attenuation of the signal power during its travel from the transmitter to the receiver due to the environment -noise errors-, the uncertainties caused by the instabilities of the measurement clocks and the occurrence of multipath must then be considered [16].

These errors are closely related to the spatial distribution of the system sensors, increasing the importance of this link in LPS. The minimization of these errors is a requirement in this article that allows the valuable comparison between synchronous and asynchronous positioning systems. Once its effects are minimized, the temporary measurements assume the greatest weight of the system error.

In this sense, the study of the optimized location of the sensors with the objective of minimizing these uncertainties in the calculation of the position has been fully studied recently.

Tekdas and Isler [17] and subsequently Yoon and Kim [18] classified the problem of optimizing the distribution of sensors for positioning within the NP-hard category, which constitutes the absence of exact algorithms that resonate in polynomial time. This circumstance has directed research in this field towards the use of metaheuristic techniques, especially Genetic Algorithms (GA) [19]–[21].

The characteristics of robustness, flexibility, optimization of non-derivable and non-linear functions and space exploration of solutions have boosted the GA as the main methodology for optimizing the distribution of sensors in LPS. Historically, the minimization of the uncertainty of the positioning was carried out based on the parameter Geometric Dilution of Position (GDOP) [22], governed by the adoption of homoscedastic noise models, where the variances have become invariants [23]. This hypothesis can be applicable in GNSS, where the distances between satellites and targets are

similar. However, this does not occur in LPS where the distances traveled by the positioning signals may vary depending on the sensor receiver.

In this regard, the Cramér-Rao Lower Bound (CRLB) allows us to know the uncertainty of the positioning based on the heteroscedastic modeling of variances in temporal measurements [24]. This characterization of the error with noise consideration is made based on the models of signal propagation losses [25] and the positioning architecture in question which supposes a key fact due to the different paths of the signals in each system.

For this purpose, in one of our previous works, we have proposed the optimization of the sensor location of LPS systems in search of the minimization of the CRLB [26]. This methodology uses a GA to locate the components of the positioning system in any type of environment, regardless of its geometric characteristics and the predefined restrictions on the location of sensors.

This previous methodology contemplates one of the main causes of uncertainty in the calculation of the position as a result of the path traveled by the signals through the different locations of the system sensors. In this article, we will complete this error model with the contribution of errors caused by the temporary instabilities of the measurement clocks in the CRLB model.

This error characterization is mixing the uncertainties from the signal propagation, which are greater in A-TDOA rather than in TDOA and TOA systems as a consequence of the architecture design -the signal paths are greater-, and the clock errors which are reduced in A-TDOA systems rather than in TDOA and TOA as a consequence of the elimination of the synchronism. This fact promotes that only in scenarios where optimization has been performed, the time-based positioning systems accuracy achievable is comparable.

With this consideration, we apply for the first time in the authors' best knowledge a 3D optimization of the sensor location in any application environment for TOA, TDOA and A-TDOA architectures with the minimization of the positioning uncertainty induced by the combined effect of noise and system measurement clocks. We develop this methodology and this error modeling in order to be able to perform an a priori comparison of the suitability of each architecture in a 3D complex environment and in order to show the effects of the synchronization process in the combined errors of each system.

The remainder of the article is organized as follows: in Section 2 the notation is introduced and the mathematical models of temporal instabilities of the measurement clocks for the TOA, TDOA and A-TDOA architectures are presented. Section 3 shows the construction of the CRLB to model the effects of noise and clock errors. Section 4 develops aspects related to the generation of the fitness function of the GA optimization required for the valuable comparison between architectures. Section 5 shows the results of the proposed methodology. Finally, sections 6 present the advances in innovation and the research conclusions.

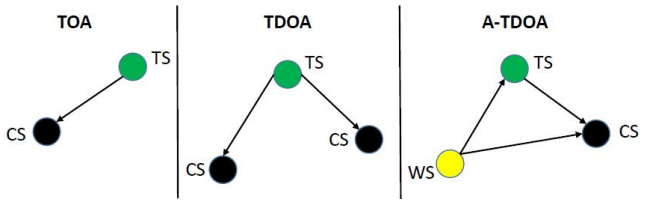

FIGURE 1. Sensor notation for TOA, TDOA and A-TDOA architectures.

II. INFLUENCE OF CLOCK ERRORS IN LPS

In this section, a characterization of time measurement errors induced by clocks in terms of positioning architectures is presented. The notation used throughout the study is described hereafter. Target Sensor (TS) indicates the target location. Coordinate Sensor (CS) represents every sensor of TOA, TDOA or A-TDOA methodologies that are capable of performing time measurements. In the case of TOA and TDOA architectures, all sensors will be CS, whereas in the A-TDOA technique [14] only one of them will possess the time measurement device. The term Worker Sensors (WS) refers to all architecture sensors without the capability of measure, acting as transponders. Lastly, N_{CS} is the number of CS and N_{WS} the number of WS. The described notation is presented in Figure 1 for TOA, TDOA and A-TDOA architetures.

Temporal instabilities in clocks originate from the appearance of additional uncertainties in time measurements during the location process. Zhou *et al.* [13] model clock errors according to two parameters: initial-time offset and clock drift. The initial-time offset points out the temporal delay between the reference clock used for synchronization and the clock located in every CS of positioning architectures. Thus, this error only appears when a synchronization process is needed. The clock drift indicates the frequency deviation of the clocks, which introduces a cumulative error during time measurements. Conventionally, this clock instability is expressed in parts-per-million (ppm) or parts-per-billion (ppb).

The presence of initial-time offsets and/or clock drifts disturb time measurements in every time-based positioning methodology. However, their influence on final location accuracy depends on architecture characteristics, meaning that certain techniques are more vulnerable to these errors.

In the next paragraphs, an analysis of clock errors in time measurements of TOA ($\mathbf{T_{TOA}}$), TDOA ($\mathbf{T_{TDOA}}$) and A-TDOA ($\mathbf{T_{A-TDOA}}$) architectures is presented. This enables the modeling of these uncertainties and the collection of relationships between clock errors and the location of sensors in every architecture.

Zhou *et al.* [13] characterize the time measurement perturbed by clock instabilities as:

$$t = t' + U + \eta(t' - M) \tag{1}$$

where t indicates the clock measurement, t' indicates the ideal time measurement, U is the initial-time offset, η is the

clock drift and M specifies the instant of the last process of synchronization.

Based on this error description, uncertainties in time measurements are obtained for each architecture on analysis. Firstly, relations that governed TOA methodology are presented:

$$\begin{aligned} T_{TOAi} &= t_i - t_0 \\ T_{TOAi} &= \left[t_i^{'} + U_i + \eta_i\left(t_i^{'} - M\right)\right] \\ &\quad - \left[t_0^{'} + U_0 + \eta_0\left(t_0^{'} - M\right)\right] \quad i = 1, \ldots, N_{CS} \end{aligned} \tag{2}$$

where the i sub-index refers to time measurements of each TOA sensor and the *0* sub-index indicates those measures carried out by the TS. Ideal time measurements are defined – $t_i^{'}$ and $t_0^{'}$– in the following equations:

$$t_i^{'} = t_0^{'} + \|TS - CS_i\|/_c = M + T_0 + T_i \quad t_0^{'} = M + T_0 \tag{3}$$

where T_0 is the interval between the end of the synchronization process and the instant of the positioning pulse emission, and T_{i} is the amount of time required by the positioning signals to flight from the target to each CS of TOA architectures. In addition to the characterization of clocks instabilities, the temporal resolution of the implemented clocks must be considered. For this purpose, each TOA time measurement is truncated ($floor_{TR}$) based on the clock parameters of resolution.

$$\begin{aligned} T_{TOAi} &= T_i + U_i - U_0 + T_0\left(\eta_i - \eta_0\right) + T_i\eta_i \\ CE_{TOA_i} &= \left|T_i - floor_{TR}\left(T_{TOA_i}\right)\right| \end{aligned} \tag{4}$$

where $\mathbf{T_{TOA}}$ and $\mathbf{CE_{TOA}}$ are respectively the actual time measurement and the clock error in each TOA sensor. In the case of a TDOA architecture, time measurements with the effect of clock errors are characterized in terms of the next relations:

$$\begin{aligned} T_{TDOA_{ij}} &= (t_i - t_0) - \left(t_j - t_0\right) = t_i - t_j \\ T_{TDOA_{ij}} &= \left[t_i^{'} + U_i + \eta_i\left(t_i^{'} - M\right)\right] \\ &\quad - \left[t_j^{'} + U_j + \eta_j\left(t_j^{'} - M\right)\right] \\ &\quad i = 1, \ldots, N_{CS} \\ &\quad j = 1, \ldots, N_{CS} \\ &\quad where \;\; i \neq j \end{aligned} \tag{5}$$

where ideal time measurements in each sensor– t_i' and t_j'– are derived from the architecture characteristics:

$$\begin{aligned} t_i^{'} &= t_0^{'} + \|TS - CS_i\|/_c = M + T_0 + T_i \\ t_j^{'} &= t_0^{'} + \left\|TS - CS_j\right\|/_c = M + T_0 + T_j \end{aligned} \tag{6}$$

where T_{i} and T_j represent the time interval associated with the travel of the positioning signal from the target to each CS of TDOA architectures. Inserting "(6)" in "(5)" and adding the truncating effect derived from the deployment of clocks with finite time resolution:

$$\begin{aligned} T_{TDOA_{ij}} &= [T_i + U_i - U_0 + T_0\left(\eta_i - \eta_0\right) + T_i\eta_i] \\ &\quad - \left[T_j + U_j - U_0 + T_0\left(\eta_j - \eta_0\right) + T_j\eta_j\right] \\ T_{TDOA_i} &= [T_i + U_i - U_0 + T_0\left(\eta_i - \eta_0\right) + T_i\eta_i] \\ T_{TDOA_j} &= \left[T_j + U_j - U_0 + T_0\left(\eta_j - \eta_0\right) + T_j\eta_j\right] \\ CE_{TDOA_{ij}} &= \left|T_i - floor_{TR}\left(T_{TDOA_i}\right)\right| \\ &\quad + \left|T_j - floor_{TR}\left(T_{TDOA_j}\right)\right| \end{aligned} \tag{7}$$

where $\mathbf{T_{TDOA}}$ and $\mathbf{CE_{TDOA}}$ represent the TDOA time measurement and the concerning error in each TDOA measure. Time measurements uncertainties originated by clock errors in A-TDOA architecture [12], [14] are modeled by the following equations:

$$\begin{aligned} T_{A-TDOA_i} &= (t_i - t_0) - (t_{CS} - t_0) = t_i - t_{CS} \\ T_{A-TDOA_i} &= \left[t_i' + U_{CS} + \eta_{CS}\left(t_i' - M\right)\right] \\ &\quad - \left[t_{CS}' + U_{CS} + \eta_{CS}\left(t_{CS}' - M\right)\right] \\ &\quad i = 1, \ldots, N_{WS} \end{aligned} \tag{8}$$

where time measurements based on ideal conditions and in the absence of error – t_i' and t_{CS}'– are modeled through the following relations:

$$\begin{aligned} t_i' &= t_0^{'} + \|TS - WS_i\|/_c + \|TS - \mathrm{CS}\|/_c \\ &= M + T_0 + T_i + T_{TS} \\ t_{CS}' &= t_0^{'} + ||WS_i - CS||/_c = M + T_0 + T_{CS_i} \end{aligned} \tag{9}$$

where T_i is the time of flight from the target to each WS of A-TDOA architectures, T_{TS} is the duration that the positioning signal needs to complete the distance between the target and the CS, and T_{CS_i} is referred to the period of time from the emission of the positioning signal in each WS to its reception in the CS. Combining "(8)" and "(9)" and including the time resolution effect on the measurements:

$$\begin{aligned} T_{A-TDOA_i} &= \left(T_i + T_{TS} - T_{CS_i}\right)\left(1 + \eta_{CS}\right) \\ CE_{A-TDOA_i} &= \left|\left(T_i + T_{TS} - T_{CS_i}\right) - floor_{TR}\left(T_{A-TDOA_i}\right)\right| \end{aligned} \tag{10}$$

where $\mathbf{T_{A-TDOA}}$ and $\mathbf{CE_{A-TDOA}}$ refer to the time measurement of each A-TDOA pair of sensors and the error introduced due to the clock instabilities.

Previous expressions reveal the key importance of the travel carried out by the positioning signal in the magnitude of the absolute error of time measurement uncertainties due to clock errors. However, their relativity on the final measure varies in function of the positioning architecture. This phenomenon is modeled by the Clock Relative Error (CRE), which is the ratio of absolute time error to ideal time measurement ignoring the time resolution. This is due to the independency of this factor with location methodologies:

$$CRE_{TOA_i} = \frac{\left|U_i - U_0 + T_0\left(\eta_i - \eta_0\right) + T_i\eta_i\right|}{T_i} \tag{11}$$

$$\begin{aligned} CRE_{TDOA_{ij}} &= \frac{\left|U_i - U_0 + T_0\left(\eta_i - \eta_0\right) + T_i\eta_i\right|}{T_i} \\ &\quad + \frac{\left|U_j - U_0 + T_0\left(\eta_j - \eta_0\right) + T_j\eta_j\right|}{T_j} \end{aligned} \tag{12}$$

$$CRE_{A-TDOA_i} = \frac{|\eta_{CS}|\,|T_i + T_{TS} - T_{CS}|}{|T_i + T_{TS} - T_{CS}|} = |\eta_{CS}| \tag{13}$$

These equations expose an important conclusion. CRE in A-TDOA architectures is constant and it only depends on CS clock frequency drift. In other words, the relativity of the clock errors in the final time measurement does not depend on sensors or target location. In contrast, in TOA and TDOA methodologies the impact of clock uncertainties is dependent on the signal travel and all clock instabilities.

Based on this analysis, the minimization of absolute temporal uncertainties and their influence on final measures is possible through an optimization of the distribution of the sensors of time-based positioning architectures. It is interesting to highlight that this effect is accomplished by the direct minimization of the time measurements performed by the CS clock in A-TDOA methodologies.

III. CRLB DERIVATION WITH CLOCK ERRORS IMPLEMENTATION

CRLB implementation in positioning enables the determination of the maximum accuracy of location when temporal measurements are perturbed. This tool has been widely adopted for LOS and NLOS conditions, as shown in [27]. The suitability of the CRLB, especially for LPS relies on the heteroscedasticity of variance models, heterogeneity in the sensor placement circumstances, and flexibility in the characterization of several operating conditions.

Conventionally, this technique has been used to characterize the reduction of accuracy in location due to time measurement errors induced by noise. The presence of noise in the communication channel has been traditionally modeled by a White Gaussian Noise (WGN) distribution [28]. Based on this assumption, Kaune *et al.* [29] develop a generic matrix form of CRLB where time measurement uncertainties are dependent on target-sensor distance [14], [26].

$$J_{mn} = \left(\frac{\partial h\,(TS)}{\partial x_m}\right)^T R^{-1}\,(TS)\left(\frac{\partial h\,(TS)}{\partial x_n}\right) + \frac{1}{2}tr\left(R^{-1}(TS)\left(\frac{\partial R\,(TS)}{\partial x_m}\right)R^{-1}\,(TS)\left(\frac{\partial R\,(TS)}{\partial x_n}\right)\right) \tag{14}$$

In this relation, **J** is the Fisher Information matrix where m and n sub-indexes represent the parameters to estimate – TS Cartesian coordinates-. **h**(**TS**) vector indicates distance relationships between sensors and targets according to the positioning signal travel in every architecture.

$$h_{TOA_i} = \|TS - CS_i\| \quad i = 1, \ldots, N_{CS} \tag{15}$$

$$h_{TDOA_i} = \|TS - CS_i\| - \left\|TS - CS_j\right\| \quad i = 1, \ldots, N_{CS}\ \ j = 1, \ldots, N_{CS} \tag{16}$$

$$h_{A-TDOA_i} = ||TS - WS_i|| + ||TS - CS|| - ||WS_i - CS|| \quad i = 1, \ldots, N_{WS} \tag{17}$$

The quantification of uncertainties in each time measurement is performed through the covariance matrix **R** (**TS**). In this paper, a combined model of noise effects and clock errors is presented based on the assumption of independence between these two factors. Reasons for this hypothesis rest in the absence of relation between the physical source of these disruptions.

The construction of the **R** (**TS**) matrix is subjected to significant differences according to positioning architectures. In the case of TOA and A-TDOA time measurements are independent of each other. In contrast, Z. Sahinoglu *et al.* proved in [30] that TDOA time differences measurements are correlated, which causes the presence of non-zero off-diagonal terms in the covariance matrix.

Noise components of variances in the **R** (**TS**) matrix is built based on a heteroscedastic model that is governed by a Log-normal path-loss propagation model. This characterization has been made under the assumption of uncorrelated measurement noise at different sensors [29]:

Clock error terms in **R** (**TS**) matrix has been defined based on Monte-Carlo simulation of l iterations in order to correctly estimate each temporal variance associated with every positioning architecture. In addition, the time resolution is introduced in order to maximize clock uncertainty representation. The combined expressions of variances for noise and clock errors are presented in the following equations:

$$\sigma^2_{TOA_i} = \frac{c^2}{B^2\left(P_T/P_n\right)}PL\,(d_0)\left[\left(\frac{d_i}{d_0}\right)^n\right] + \frac{1}{l}\sum_{k=1}^{l}\left\{CE_{TOA_i}c\right\}^2$$
$$d_i = \|TS - CS_i\| \quad i = 1, \ldots, N_{CS} \tag{18}$$

$$\sigma^2_{TDOA_{ij}} = \frac{c^2}{B^2\left(P_T/P_n\right)}PL\,(d_0)\left[\left(\frac{d_i}{d_0}\right)^n + \left(\frac{d_j}{d_0}\right)^n\right] + \frac{1}{l}\sum_{k=1}^{l}\left\{CE_{TDOA_{ij}}c^2\right\}$$
$$d_i = \|TS - CS_i\|$$
$$d_j = \left\|TS - CS_j\right\| \quad i = 1, \ldots, N_{CS}\ j = 1, \ldots, N_{CS}\ \ where\ i \neq j \tag{19}$$

$$\sigma^2_{A-TDOA_i} = \frac{c^2}{B^2\left(P_T/P_n\right)}PL\,(d_0) \times \left[\left(\frac{d_i}{d_0}\right)^n + \left(\frac{d_{TS}}{d_0}\right)^n + \left(\frac{d_{CS}}{d_0}\right)^n\right] + \frac{1}{l}\sum_{k=1}^{l}\left\{CE_{A-TDOA_i}c\right\}^2$$
$$d_i = \|TS - WS_i\|$$
$$d_{TS} = ||TS - \mathrm{CS}||$$
$$d_{CS_i} = ||WS_i - CS|| \quad i = 1, \ldots, N_{WS} \tag{20}$$

where c is the signal propagation speed in m/s, B is the signal bandwidth is Hz, P_T is the transmission power

in W, P_n is the mean noise level in W which is calculated based on Johnson-Nyquist relation, n is the path loss exponent, d_0 is the reference distance for the Log-normal model, $PL(d_0)$ is the path-loss related to reference distance.

Lastly, global accuracy in positioning is evaluated by means of the Mean Squared Error (MSE) of diagonal elements of matrix $\mathbf{J}^{-1}$. This enables an incremental penalization when the accuracy reduces its magnitude, which helps in the optimization process.

IV. FITNESS FUNCTION MODELING

In the previous sections, a combined clock and noise error model has been introduced in order to consider the uncertainties of the measurement devices and the signal deterioration in positioning systems. This model can be applied to achieve an optimized node distribution in TOA, TDOA and A-TDOA systems through the minimization of these uncertainties in each architecture. This is the main goal of this article and must guarantee the reduction of global positioning errors in any navigation environment for any type of vehicle.

The achievement of these objectives has led to the application of the positioning sensor layout proposed by J. Díez-González *et al.* [26]. This procedure is based on a Genetic Algorithm (GA) that allows the optimization of sensor placement in 3D irregular environments with free definitions of the reference surface and the region of optimization. For this purpose, the GA employs a methodology that allows the transformation of the cartesian coordinates of each individual in the population from binary to real digits –and vice versa– according to the local characteristics of the optimization environments. Additionally, this GA provides freedom in the choice of: the selection technique –Tournament 2, Tournament 3, Roulette and Ranking–, the percentage of elitism and mutation, and the convergence criteria. Finally, a partial process of resolution allows the progressive reduction of the space of solution, stimulating the intensification in the search of the final solution.

Once the algorithm has been defined, the fitness function selection is the key factor to perform the optimization process. In this case, the fitness function must allow the combined reduction of the uncertainties introduced by noise and clock errors, with the aim of reaching the highest levels of accuracy for each positioning architecture. The equations defined in the Sections 2 and 3, show that a minimization of the signal travel, and the reduction of the time measurements in each clock -without null measurements- in order to minimize the influence of the clocks in the global error, allows the optimization of the global process with a concrete number of sensors.

This optimization methodology has led to the maximization of the inverse of the mean values of the Mean Squared Error (MSE) measured in each possible vehicle location in the optimization environment as follows. In addition, the fitness function penalizes forbidden sensor locations pre-determined based on environment characterization.

$$ff = \frac{1}{mean\,(MSE_{NT})} - C_P \frac{\sum_{i=1}^{N} R_i}{N} \tag{21}$$

where NT indicates the total number of evaluation points of the CRLB, N is the total number of architecture sensors, R_i represents the existence or not -1, 0 respectively- of sensors located in a banned area, and C_P is the weight associated to the penalization factor.

V. RESULTS

In this section, the accuracy results after the optimization of sensors located in a 3D irregular environment for TOA, TDOA and A-TDOA architectures are presented.

Firstly, a 3D irregular scenario has been designed for the simulations. Area designations have followed the considerations of [26]. This simulation environment has been selected in order to exemplify a possible situation of optimization in real conditions. In this way, NLE is the Node Location Environment which indicates the extension free movement of the sensors during optimization, and TLE is the Target Location Environment which represents all possible locations of the positioning targets.

As can be observed in Figure 1, the NLE region spreads throughout the base surface with the exception of the zone corresponding to the TLE projection over the surface. In terms of elevation, the NLE minimum height is 1 meter - to prevent non-modeling events like multipath - and the maximum elevation is pre-set to 15 meters to restrict sensor environment disruption. The NLE region resolution is contained in the interval [0.5,1] meters due to the adaptability of the length of the GA chromosomes based on the environment extension.

In the case of the TLE zone, limiting levels are 1 meter as the minimum and 120 meters as maximum. They have been selected to represent a joint aerial-ground accuracy maximization with maximum representativeness of the reality-based on pre-establish assumptions. The spatial discretization of the TLE region is 30 meters on x and y Cartesian coordinates, and 5 meters on z coordinate. This provides sufficient spatial resolution for the optimization, without reducing significantly the number of studied points.

Once the optimization scenario is selected, the next step is the determination of global configuration parameters that allow the comparison among time-based positioning architectures.

Lastly, the GA configuration parameters selected are Tournament 3 as selection procedure, 7 % of elitism, single-point crossover and mutation probability of 3 %. This election provides the best relation between fitness function maximization and convergence speed. It must be stressed that TDOA and A-TDOA optimization have been carried out with five sensors in order to deploy the minimum number of them to accomplish and univocal 3D positioning. In the case of TOA architecture, the optimization process has been performed

TABLE 1. TOA, TDOA and A-TDOA architectures parameters for optimization. Variables selection for noise modeling has been accomplished based on [31], whereas clock errors characterization is in reliance with [13].

Parameter	Value
Transmission power	400 W
Mean noise power	- 94 dBm
Frequency of emission	1090 MHz
Bandwidth	100 MHz
Clock frequency	1 GHz
Frequency-drift	$U\{-10, 10\}$ ppm
Initial-time offset	$U\{15, 30\}$ ns
Time from synchronization	1 μs
Path loss exponent	2.1
Antennae gains	Unity
Time-Frequency product	1
Communication type	Full-duplex

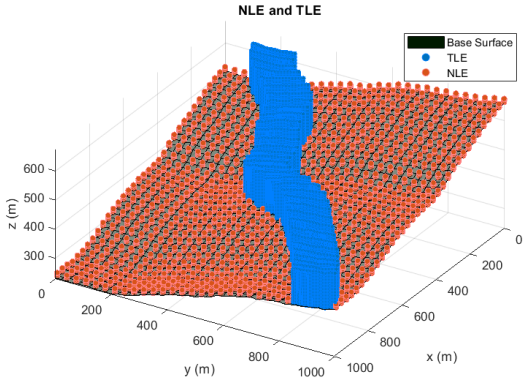

FIGURE 2. The scenario of the simulations. 3D irregular environment characterization for node optimization distribution of sensors in TOA, TDOA and A-TDOA architectures.

with four and five sensors to facilitate the comparison and the acquisition of conclusions.

The importance of the sensor placement for any positioning architecture is proved in Figure 2, where the CRLB is obtained for a random distribution of 5 sensors for TOA architecture.

As shown, a non-optimized location of sensors is the major contribution to the increase in the uncertainty of positioning. The accuracy evaluation after the optimization of sensor location for TOA, TDOA and A-TDOA architectures with noise and clock error uncertainties, is presented hereafter. Results are shown together with the localization of the optimized sensor placement in the environment.

A comparative in terms of accuracy is displayed in Tables 2 and 3 for all positioning methodologies on analysis. These values have been obtained based on five different optimizations for each architecture with the objective of

TABLE 2. Accuracy analysis for TOA, TDOA and A-TDOA architectures after sensor location optimization when noise uncertainties are present. Values in parentheses indicate the number of sensors in the distribution.

CRLB: Noise	TOA (4)	TOA (5)	TDOA (5)	A-TDOA (5)
Mean (m)	0.336	0.253	0.303	0.640
Max (m)	2.204	0.774	1.964	2.352
Min (m)	0.147	0.053	0.091	0.119
% < 0.5 m	84.74	92.16	84.06	52.47

TABLE 3. Accuracy analysis for TOA, TDOA and A-TDOA methodologies after sensor location optimization when noise and clock error uncertainties are considered. Values in parentheses indicate the number of sensors in the distribution.

CRLB: Noise + Clock errors	TOA (4)	TOA (5)	TDOA (5)	A-TDOA (5)
Mean (m)	19.993	17.962	8.152	0.704
Max (m)	77.377	44.480	24.129	3.277
Min (m)	8.761	7.177	3.124	0.130
% < 0.5 m	0	0	0	44.80
% Clock /Total errors	97.86	98.22	95.72	34.74

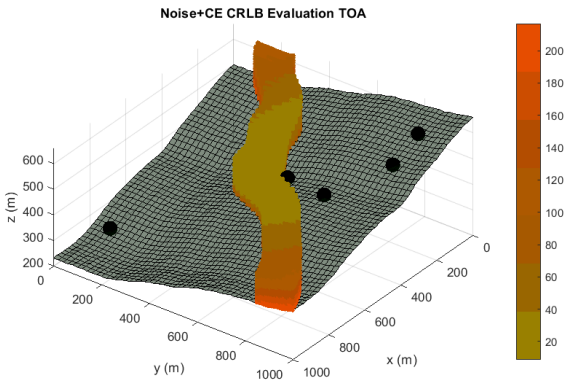

FIGURE 3. RMSE analysis in terms of noise and clock errors for TOA architecture with 5 sensors. The distribution of sensors is not optimized via GA. The reference surface is presented in grey tones. Black spheres symbolize the localization of each sensor.

avoiding peak results due to the random initialization of the GA. Firstly, results are shown when only noise effects affect the time measurements.

Secondly, accuracy estimation with noise and clock error uncertainties is evaluated for positioning architectures.

Tables 2 and 3 reveal important information about the performance of the architectures in the analysis for an LPS application. Synchronous methodologies –TOA and TDOA- provide better accuracy than asynchronous (A-TDOA) if only noise disturbance is modeled. This aspect is directly related to the reduction of the travel distance of positioning signal which is typical of TOA and TDOA methods.

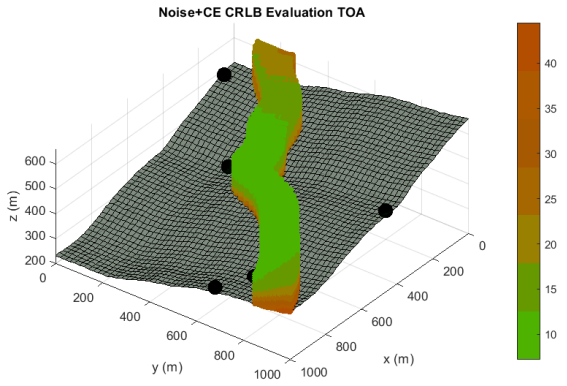

FIGURE 4. RMSE analysis in terms of noise and clock errors for TOA architecture with an optimized node distribution of 5 sensors.

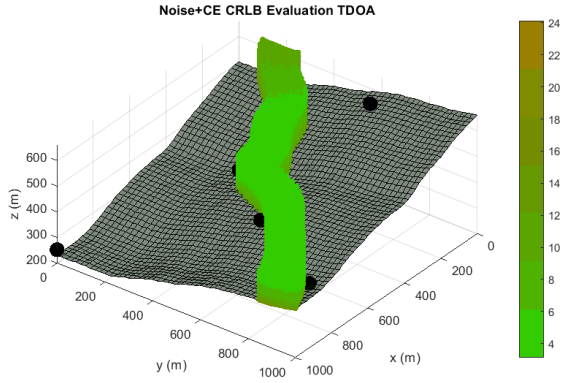

FIGURE 5. RMSE analysis in terms of noise and clock errors for TDOA architecture with an optimized node distribution of 5 sensors.

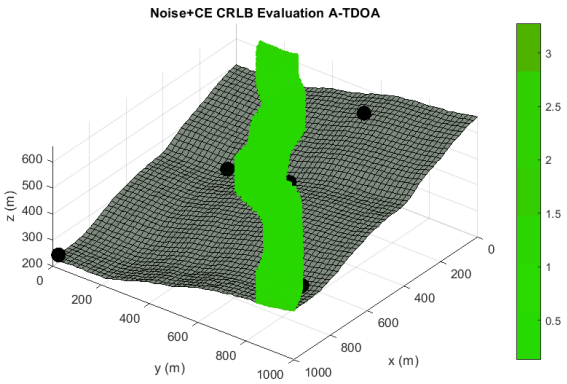

FIGURE 6. RMSE analysis in terms of noise and clock errors for A-TDOA architecture with an optimized node distribution of 5 sensors.

However, when clock instabilities are added to noise as uncertainty factors in time measurements, the performance of A-TDOA architecture is far significantly higher than synchronous methodologies. This is mainly induced by the elimination of initial time-offset and cumulative errors that are introduced in the time measurements as a consequence of the time-lapse from the last synchronization. In addition, A-TDOA architectures could reduce, through the sensor distribution, the amount of the time measurements thanks to the TDOA methodology employing one common sensor (CS) for all measures. Clock error models have shown that this aspect directly reduces the uncertainties induced in the final

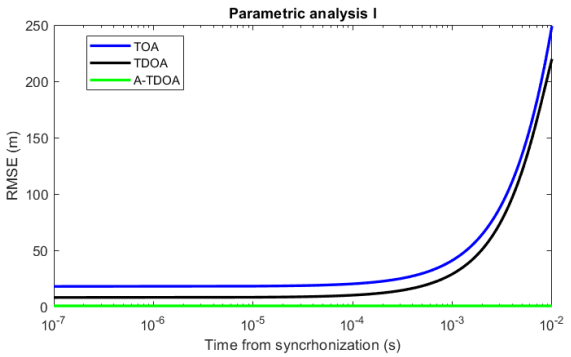

FIGURE 7. Parametric analysis of the time from synchronization in TOA, TDOA and A-TDOA architectures with an optimized distribution of 5 sensors. Variables for the analysis are derived from Table 1.

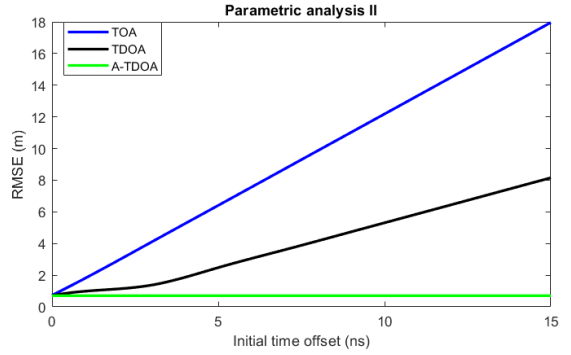

FIGURE 8. Parametric analysis of initial time offset for TOA, TDOA and A-TDOA architectures with an optimized distribution of 5 sensors. Variables for the analysis are derived from Table 1.

measurement, and the errors in the final positioning. The relation of these magnitudes with the global accuracy for TOA, TDOA and A-TDOA architectures are presented hereafter:

Figure 6 and 7 reveals that TOA and TDOA architectures would provide the same accuracy level if their sensors initial-time offset were null and the time from synchronization was less than 1 μs, which is nearly impracticable with actual technology. Based on these results, the better candidate in terms of accuracy and performance stability for LPS applications are the asynchronous time-based architectures.

VI. CONCLUSION

The LPS have emerged as the most adequate systems for high-performance applications in terms of accuracy and stability in the target localization. This has been achieved through the reduction of the uncertainties related to the measurements in these architectures and the flexibility to locate the sensor distribution in the space.

In this paper, we have developed for the first time in the authors' best knowledge a model to consider the uncertainties introduced by the navigation environment and the clock instabilities in the time measurements of the CRLB matrix. This methodology has been derived for the TOA, TDOA and A-TDOA architectures, with the aim of evaluating their performance based on a set of global communication parameters under a 3D-real environment. This error characterization

shows the necessary process to minimize these measurement instabilities and jointly reduce the influence of the signal travel.

It must be highlighted that it has been shown that the Clock Relative Error (CRE) in A-TDOA architectures has a constant factor that is independent of the signal positioning travel and it only depends on the clock drift of its coordinate sensor which produces great stability in the accuracy results of this methodology. This fact has special relevance in LPS where distances between target and sensors are highly heterogeneous.

The minimization of the error uncertainties requires an optimized sensor distribution for each architecture in order to make the results comparable and to achieve practical results. This is a consequence of the influence of the sensor deployment in the signal paths of each architecture as well as time lapses to be measured. In optimized sensor distributions signal paths are reduced in TOA systems from TDOA systems which in turn are smaller than A-TDOA as a result of the architecture design. But, in these systems, the path degradation of the signals can be offset by less affected clock errors. For this reason, this article studies the combined effect of these error sources under optimized node deployments for each time-based positioning architecture.

We apply a heuristic optimization for each system with the minimum number of sensors to achieve an unequivocal target location. This optimization has been achieved by means of a genetic algorithm with total independence from the space surface to locate sensors, the target possible localizations and the adoption of crossing, selection and mutation techniques.

Results show that A-TDOA provides significantly better performance in terms of accuracy and stability than TOA and TDOA architectures. The influence of the time since the last synchronization and initial time offset on clock errors have been demonstrated through a parametric analysis. A-TDOA architectures accuracy is more stable due to the elimination of uncertainties related to the synchronism process and the combined minimization of positioning signal path and time measures made by sensor clocks.

REFERENCES

[1] K. W. Kolodziej and J. Hjelm, *Local Positioning Systems: LBS Applications and Services*. Boca Raton, FL, USA: CRC Press, 2017.
[2] A. A. D'Amico, U. Mengali, and L. Taponecco, "TOA estimation with the IEEE 802.15.4a standard," *IEEE Trans. Wireless Commun.*, vol. 9, no. 7, pp. 2238–2247, Jul. 2010.
[3] T.-K. Le and N. Ono, "Closed-form and near closed-form solutions for TDOA-based joint source and sensor localization," *IEEE Trans. Signal Process.*, vol. 65, no. 5, pp. 1207–1221, Mar. 2017.
[4] J. Xu, M. Ma, and C. L. Law, "AOA cooperative position localization," in *Proc. IEEE Global Telecommun. Conf. (GLOBECOM)*, New Orleans, LO, USA, Nov./Dec. 2008, pp. 1–5.
[5] G. Wang and K. Yang, "A new approach to sensor node localization using RSS measurements in wireless sensor networks," *IEEE Trans. Wireless Commun.*, vol. 10, no. 5, pp. 1389–1395, May 2011.
[6] D. Lindgren, G. Hendeby, and F. Gustafsson, "Distributed localization using acoustic Doppler," *Signal Process.*, vol. 107, pp. 43–53, Feb. 2015.
[7] L. Taponecco, A. A. D'Amico, and U. Mengali, "Joint TOA and AOA estimation for UWB localization applications," *IEEE Trans. Wireless Commun.*, vol. 10, no. 7, pp. 2207–2217, Jul. 2011.
[8] B. Sackenreuter, N. Hadaschik, M. Fassbinder, and C. Mutschler, "Low-complexity PDoA-based localization," in *Proc. Int. Conf. Indoor Positioning Indoor Navigat. (IPIN)*, Alcalá de Henares, Spain, Oct. 2016, pp. 1–6.
[9] Y. Ma, B. Wang, S. Pei, Y. Zhang, S. Zhang, and J. Yu, "An indoor localization method based on AOA and PDOA using virtual stations in multipath and NLOS environments for passive UHF RFID," *IEEE Access*, vol. 6, pp. 31772–31782, 2018.
[10] B. Sundararaman, U. Buy, and A. D. Kshemkalyani, "Clock synchronization for wireless sensor networks: A survey," *Ad Hoc Netw.*, vol. 3, no. 3, pp. 281–323, May 2005.
[11] J. Y. D. Elson Estrin, "Time synchronization for wireless sensor networks," in *Proc. 15th Int. Parallel Distrib. Process. Symp.*, San Francisco, CA, USA, 2000, p. 1.
[12] S. He and X. Dong, "High-accuracy localization platform using asynchronous time difference of arrival technology," *IEEE Trans. Instrum. Meas.*, vol. 66, no. 7, pp. 1728–1742, Jul. 2017.
[13] J. Zhou, L. Shen, and Z. Sun, "A new method of D-TDOA time measurement based on RTT," in *Proc. MATEC Web Conf.*, vol. 207, 2018, Art. no. 03018.
[14] R. Álvarez, J. Díez-González, E. Alonso, L. Fernández-Robles, M. Castejón-Limas, and H. Perez, "Accuracy analysis in sensor networks for asynchronous positioning methods," *Sensors*, vol. 19, no. 13, p. 3024, Jul. 2019.
[15] P. Wu, S. Su, Z. Zuo, X. Guo, B. Sun, and X. Wen, "Time difference of arrival (TDoA) localization combining weighted least squares and firefly algorithm," *Sensors*, vol. 19, no. 11, p. 2554, Jun. 2019.
[16] S. Lanzisera, D. Zats, and K. S. J. Pister, "Radio frequency time-of-flight distance measurement for low-cost wireless sensor localization," *IEEE Sensors J.*, vol. 11, no. 3, pp. 837–845, Mar. 2011.
[17] O. Tekdas and V. Isler, "Sensor placement for triangulation-based localization," *IEEE Trans. Autom. Sci. Eng.*, vol. 7, no. 3, pp. 681–685, Jul. 2010.
[18] Y. Yoon and Y.-H. Kim, "An efficient genetic algorithm for maximum coverage deployment in wireless sensor networks," *IEEE Trans. Cybern.*, vol. 43, no. 5, pp. 1473–1483, Oct. 2013.
[19] J. O. Roa, A. R. Jiménez, F. Seco, C. Prieto, J. Ealo, and F. Ramos, "Primeros resultados en la optimizacion de la ubicacion de balizas para localizacion utilizando algoritmos geneticos," in *Proc. 24th Jornadas Automática*, 2005, pp. 75–86.
[20] J. O. Roa, A. R. Jiménez, and F. Seco, "Un método herurístico basado en algoritmos genéticos para optimizar la ubicación de balizas en sistemas de localización," in *Proc. 24th Jornadas de Automática*, 2006, pp. 120–129.
[21] J. Díez-González, R. Álvarez, L. Sánchez-González, L. Fernández-Robles, H. Pérez, and M. Castejón-Limas, "3D Tdoa problem solution with four receiving nodes," *Sensors*, vol. 19, no. 13, p. 2892, Jul. 2019.
[22] W. Huihui, Z. Xingqun, and Z. Yanhua, "Geometric dilution of precision for GPS single-point positioning based on four satellites," *J. Syst. Eng. Electron.*, vol. 19, no. 5, pp. 1058–1063, Oct. 2008.
[23] N. Rajagopal, S. Chayapathy, B. Sinopoli, and A. Rowe, "Beacon placement for range-based indoor localization," in *Proc. Int. Conf. Indoor Positioning Indoor Navigat. (IPIN)*, Alcalá de Henares, Spain, Oct. 2016, pp. 1–8.
[24] B. Huang, L. Xie, and Z. Yang, "TDOA-based source localization with distance-dependent noises," *IEEE Trans. Wireless Commun.*, vol. 14, no. 1, pp. 468–480, Jan. 2015.
[25] T. S. Rappaport, *Wireless Communications—Principles and Practice*. Upper Saddle River, NJ, USA: Prentice-Hall, 2002.
[26] J. Díez-González, R. Álvarez, D. González-Bárcena, L. Sánchez-González, M. Castejón-Limas, and H. Perez, "Genetic algorithm approach to the 3D node localization in TDOA systems," *Sensors*, vol. 19, no. 18, p. 3880, Sep. 2019.
[27] Y. Qi and H. Kobayashi, "Cramér–Rao lower bound for geolocation in non-line-of-sight environment," in *Proc. IEEE Int. Conf. Acoust. Speech Signal Process.*, May 2002, pp. III-2473–III-2476.
[28] B. Huang, L. Xie, and Z. Yang, "Analysis of TOA localization with heteroscedastic noises," in *Proc. 33rd Chin. Control Conf.*, Nanjing, China, Jul. 2014, pp. 327–332.
[29] R. Kaune, J. Hörst, and W. Koch, "Accuracy analysis for TDOA localization in sensor networks," in *Proc. 14th Int. Conf. Inf. Fusion*, Chicago, IL, USA, Jul. 2011, pp. 1–8.
[30] Z. Sahinoglu, S. Gezici, and I. Gvenc, *Ultra-Wideband Positioning Systems*. New York, NY, USA: Cambridge Univ. Press, 2008.
[31] A. S. Yaro and A. Z. Sha'ameri, "Effect of path loss propagation model on the position estimation accuracy of a 3-dimensional minimum configuration multilateration system," *Int. J. Integr. Eng.*, vol. 10, no. 4, pp. 35–42, 2018.

RUBÉN ÁLVAREZ was born in León, Spain, in 1994. He received the B.S. degree in aerospace engineering and the M.S. degree in aeronautical engineering from the University of León, in 2016 and 2018, respectively, and the M.S. degree in artificial intelligence from the International University of Valencia, in 2019. He is currently pursuing the Ph.D. degree with the University of León, where his research focus is on the optimization of LPS sensor location for high accuracy applications. He is currently a Researcher with the Department of Mechanical, Computer and Aerospace Engineering, University of León. He is currently working with the Positioning Department of Drotium, where he develops a positioning system for high-accuracy navigation of autonomous vehicles.

JAVIER DÍEZ-GONZALEZ was born in León, Spain, in 1994. He received the B.S. degree in aerospace engineering and the M.S. degree in aeronautical engineering from the University of León, in 2016 and 2018, respectively, where he is currently pursuing the Ph.D. degree. His research interests are the optimization of manufacturing processes, sensor location in LPS, and the applied artificial intelligence. He has also followed the leadership program of the University Francisco de Vitoria, Madrid, where he graduated in 2017. He is currently a Researcher with the Department of Mechanical, Computer and Aerospace Engineering, University of León, where he is working as an Instructor in the area of mechanics.

LIDIA SÁNCHEZ-GONZÁLEZ received the degree in computing engineering from the University of León, Spain, in 2002, and the Ph.D. degree from the University of León, in 2007. Since 2003, she has been working at the Department of Mechanical, Computing and Aerospace Engineering, University of León, as a Lecturer in the area of computer architecture and technology. Her research interests focus on digital image processing and analysis applied to medical images and industrial processes. She is also interested in high-performance computing in order to increase the performance of a system.

HILDE PEREZ received the degree in mechanical engineering from the University of Oviedo, the degree in electrical and electronic engineering from the University of León, and the Ph.D. degree from the Polytechnic University of Madrid, obtaining the Outstanding Doctorate Award, in 2012. She is currently an Associate Professor and the Head of the Department of Mechanical, Computer and Aerospace Engineering, University of Leon. She has been involved in different national research projects in collaboration with the Polytechnic University of Madrid. Her research areas of interest are related with smart systems for manufacturing and collaborative robots for manufacturing industry, modeling and simulation of machining processes, micro-manufacturing, and high-performance machining.